Role of dopant incorporation on the magnetic properties of Ce1−xNixO2 nanoparticles: An electron paramagnetic resonance study

ARTICLE *in* JOURNAL OF APPLIED PHYSICS · APRIL 2008

Impact Factor: 2.18 · DOI: 10.1063/1.2833291

6 AUTHORS, INCLUDING:

Sushil K. Misra
Concordia University Montreal
288 PUBLICATIONS **2,222** CITATIONS
SEE PROFILE

Sergey Andronenko
Kazan (Volga Region) Federal University
60 PUBLICATIONS **259** CITATIONS
SEE PROFILE

Mark H Engelhard
Pacific Northwest National Laboratory
381 PUBLICATIONS **11,968** CITATIONS
SEE PROFILE

Role of dopant incorporation on the magnetic properties of $Ce_{1-x}Ni_xO_2$ nanoparticles: An electron paramagnetic resonance study

S. K. Misra[a),b)] and S. I. Andronenko
Department of Physics, Concordia University, 1455 de Maisonneuve Boulevard West, Montreal, Quebec H3G 1M8, Canada

M. H. Engelhard
Environmental Molecular Sciences Laboratory, Pacific Northwest National Laboratory, Richland, Washington 99352, USA

A. Thurber, K. M. Reddy, and A. Punnoose[a),c)]
Department of Physics, Boise State University, Boise, Idaho 83725, USA

(Presented on 7 November 2007; received 12 September 2007; accepted 25 October 2007; published online 15 February 2008)

Nickel doping has been found to produce weak room-temperature ferromagnetism (FM) in CeO_2. The saturation magnetization (M_s) of the chemically synthesized $Ce_{1-x}Ni_xO_2$ samples showed a maximum for $x=0.04$, above which the magnetization decreased gradually. For $Ce_{1-x}Ni_xO_2$ samples with $x \geqslant 0.04$, an activation process involving slow annealing of the sample to 500 °C increased the M_s by more than two orders of magnitude. However, no such activation effect was observed in samples with $x<0.04$. Electron paramagnetic resonance (EPR) technique has been exploited to understand (i) the gradual decrease in the FM and subsequent disappearance of FM with increase in x for $x>0.04$, and (ii) the dramatic increase in M_s in the activated $Ce_{1-x}Ni_xO_2$ samples with $x \geqslant 0.04$ and the absence of this behavior in samples with $x<0.04$. Detailed analysis by simulation of the EPR data on several as-prepared $Ce_{1-x}Ni_xO_2$ samples with $0.01 \leqslant x \leqslant 0.10$ at 5 and 300 K indicates the presence of several paramagnetic species: (i) two magnetically inequivalent Ni^{2+} ions with the ionic spin $S=1$, (ii) one Ce^{3+} ion with spin $S=1/2$, and (iii) three O_2^- defects with $S=1/2$. The spectra of the samples with $x<0.04$ are dominated by a single Ni^{2+} EPR line ascribed to dopant ions in substitutional sites, whereas in samples with $x \geqslant 0.04$, there is an additional EPR line attributed to Ni^{2+} ions occupying interstitial sites. In the activated sample with $x=0.08$, the EPR line due to the interstitial Ni^{2+} ions is completely absent, and only the line due to substitutional Ni^{2+} ions is present, suggesting that the enhanced FM arises from migration of Ni^{2+} ions from interstitial to substitutional sites. © *2008 American Institute of Physics*. [DOI: 10.1063/1.2833291]

Recent studies have shown that Ni doping produces FM in CeO_2 (Ref. 1) suggesting that this material has the potential for use in spintronic devices. It has been proposed that oxygen vacancies and substitutional incorporation of transition metal ions are important to produce FM in semiconducting and insulating oxides.[2,3] Preparation of $Ce_{1-x}Ni_xO_2$ samples in nanocrystalline powder form employs a sol-gel synthesis process with $Ce(NO_3)_3 \cdot 6H_2O$ and $Ni(NO_3)_2 \cdot 6H_2O$ precursors.[1] Weak FM behavior was observed in these samples with a maximum magnetization of 1.21 memu/g ($8.59 \times 10^{-4} \mu_B$/Ni ion) for $x=0.04$.[1] Magnetization of $Ce_{1-x}Ni_xO_2$ samples at room temperature exhibited an increase with increasing doping concentration up to 4% of Ni, followed by a decrease with further doping. There are three important experimental results of interest as far as the magnetic properties of $Ce_{1-x}Ni_xO_2$ samples are concerned.[1] (i) The observed dramatic changes in the FM behavior in the samples with $x>0.04$ are not characterized by any percolation limit,[2] (ii) considerable improvement of the weak ferromagnetic behavior of the $Ce_{1-x}Ni_xO_2$ powders with $x \geqslant 0.04$ upon slow heating of the samples to 500 °C in the presence of an externally applied magnetic field.[1] This effect, referred to hereafter as the activation process, was also reproduced recently without using an external field during the slow heating process. The M_s was found to increase by two to three orders of magnitude in these samples when subjected to the activation process, which were measured to be 0.10, 0.095, and $0.050 \mu_B$/Ni ion for 4%, 8%, and 10% Ni, respectively. (iii) The absence of the activation effect in samples with $x<0.04$. This paper deals with providing an explanation of these three behaviors by simulation of the EPR spectra of these samples to fit the experimental spectra, obtained at 5 and 300 K, in order to understand how Ni^{2+} ions are incorporated into the CeO_2 lattice and how they interact with their local environment. For relevant EPR literature on $3d$ ions, see Ref. 4.

These data are used here to identify the ionic state of the nickel ion. Figure 1(a) shows the XPS spectra displaying the Ni $2p_{3/2}$ spectral region of the $Ce_{1-x}Ni_xO_2$ samples. The general features of the Ni $2p_{3/2}$ core region of the $Ce_{1-x}Ni_xO_2$ samples and the observed peak position of ~855.1 eV are indicative of the Ni^{2+} state; the spectral parameters are clearly different from those of Ni in NiO or metallic Ni.[5–7] X-ray photoelectron spectroscopy (XPS) data of the Ce $3d_{5/2}$

[a)]Author to whom correspondence should be addressed.
[b)]Electronic mail: skmisra@alcor.concordia.ca.
[c)]Electronic mail: apunnoos@boisestate.edu.

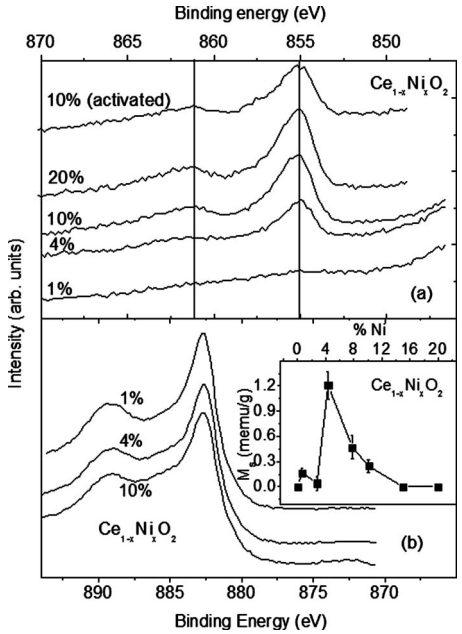

FIG. 1. XPS plots of the (a) Ni $2p_{3/2}$ region and (b) Ce $3d$ region for selected samples. Inset in (b) shows the variation of saturation magnetization with Ni concentration of as-prepared samples.

core region of $Ce_{1-x}Ni_xO_2$ samples are shown in Fig. 1(b), including a plot of M_s as function of Ni concentration. In addition to the expected signature peaks of Ce^{4+}, weaker features corresponding to approximately 15% of the cerium ions in the Ce^{3+} state are also present.[8] XPS spectrum taken from the activated samples [Fig. 1(b)] did not show any significant change in the 2+ oxidation state for Ni ions, suggesting that the observed changes in the FM properties upon activation are not due to a change in the oxidation/spin state of Ni ions.

The powder samples are comprised of nanocrystals of CeO_2 possessing the fluorite structure (space group O_h^5). When a divalent $3d$ impurity ion, such as Ni^{2+}, substitutes for the tetravalent Ce^{4+} ion in CeO_2, it causes an axial distortion due to its different size and charge from that of a Ce^{4+}

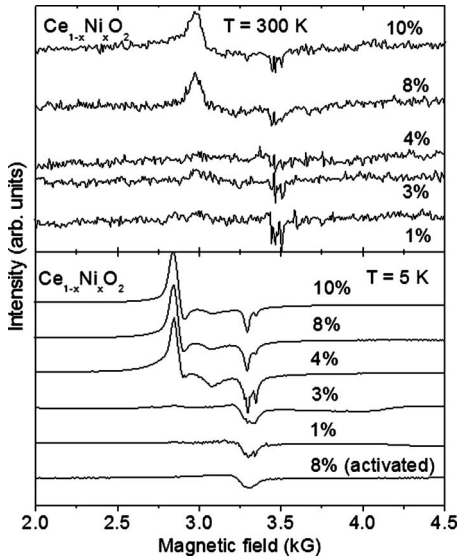

FIG. 2. Experimental X-band (9.39 GHz) EPR spectra for the various samples at 300 K (top panel) and at 5 K (bottom panel).

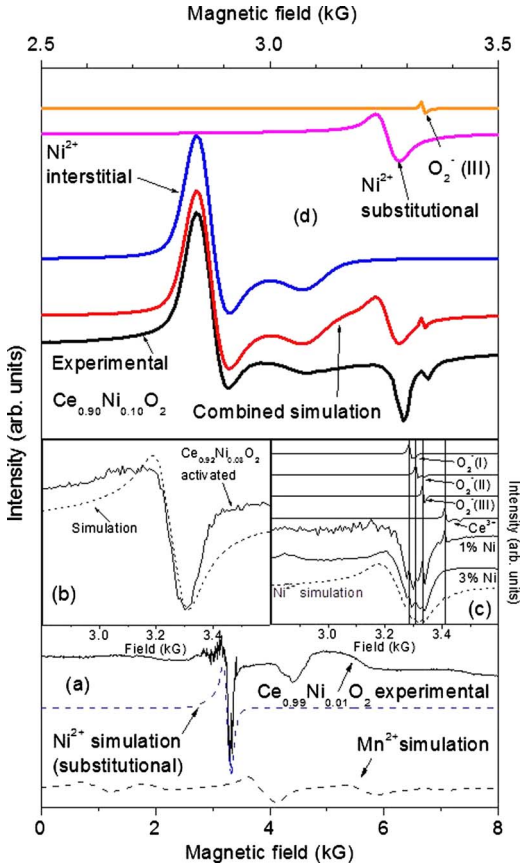

FIG. 3. (Color online) (a) Simulated Ni^{2+} (substitutional) and Mn^{2+}, and experimental EPR spectra for the sample with 1% Ni doping, showing overlap of spectra due to nickel ions at substitutional sites and that due to Mn^{2+} ions. (b) shows the simulated and experimental spectra for the activated sample with 8% Ni doping, which contains nickel ions occupying substitutional sites exclusively. (c) magnifies the details of the $g \sim 2$ region for 1% Ni-doped sample; as well it includes the simulated spectra expected for individual O_2^- defects I, II, III, and Ce^{3+} ions. (d) Simulated and experimental X-band EPR spectra for the sample with 10% Ni doping at 5 K. The individual spectra expected for nickel ions occupying interstitial and substitutional sites, as well as that due to O_2^- (III) defects are also included.

ion. Figure 2 shows the EPR spectra of $Ce_{1-x}Ni_xO_2$ samples with $0 \leqslant x \leqslant 0.10$ recorded at 300 and 5 K. The data were analyzed based on the following spin Hamiltonians (SH). For the spin $S=1/2$ state of the Ce^{3+} ion and that of the O_2^- defects the SH is $H_S=\mu_B \mathbf{B}\cdot\mathbf{g}\cdot\mathbf{S}$, representing the Zeeman interaction, with B, g, and μ_B being the magnetic-field intensity, g-matrix, and Bohr magneton, respectively. For the spin-1 state of Ni^{2+} ions the SH is $H_S=\mu_B \mathbf{B}\cdot\mathbf{g}\cdot\mathbf{S}+D[S_z^2-(1/3)S(S+1)]+E[S_x^2-S_y^2)]$, where D and E are the axial and nonaxial zero-field splitting parameters, respectively. The spectra were simulated using the WIN-EPR software (Bruker) employing an overlap of the following paramagnetic species: two inequivalent Ni^{2+}, one Ce^{3+}, and three O_2^- oxygen defects. The experimental spectra for a minority of samples with $x \leqslant 0.04$ indicated additionally the presence of trace concentrations of Mn^{2+} as an impurity. The magnetic properties of these samples did not show a significant change from those without Mn^{2+} impurity. The Mn^{2+} ion is characterized by the electron and nuclear spins $S=5/2$ and $I=5/2$, necessitating the inclusion of the hyperfine term $AS\cdot I$, where the hyperfine interaction, characterized by the parameter A, is assumed to be isotropic. Figure 3 shows the simulated

TABLE I. Spin-Hamiltonian parameters for $Ce_{1-x}Ni_xO_2$ powder. (Here L and G denote Lorentzian and Gaussian line shapes, respectively, whereas L/G is the proportion of the Lorentzian to the Gaussian line shape used for simulation. Nickel ions at substitutional and interstitial sites are indicated by I and II, respectively. The linewidths, D, E, and A are expressed in units of Gauss.)

Paramagnetic center	g_x	g_y	g_z	D	E	ΔH_x	ΔH_y	ΔH_z	Line shape	A
Ce^{2+}	1.967	1.967	1.940	⋯	⋯	5	5	5	G	⋯
O_2^- (I)	2.045	2.045	2.032	⋯	⋯	5	5	5	G	⋯
O_2^- (II)	2.030	2.030	2.010	⋯	⋯	5	5	5	G	⋯
O_2^- (III)	2.015	2.015	2.010	⋯	⋯	5	5	5	G	⋯
Ni^{2+} (I) 1%,3%	2.061	2.061	2.220	50.0	0.0	95	95	450	L	⋯
Ni^{2+} (I) 4%,8%,10%	2.061	2.061	2.220	0.0	0.0	40	40	450	L	⋯
Ni^{2+} (II) 4%,8%,10%	2.35	2.35	2.18	0.0	0.0	60	60	80	$L/G=0.01$	⋯
Mn^{2+}	2.05	2.05	2.05	1500	0.0	200	200	200	G	80

spectra representative of the experimental EPR data of $Ce_{1-x}Ni_xO_2$. To facilitate direct comparison, the experimental spectra of 1% Ni doped samples and 10% Ni doped samples are included in Figs. 3(a) and 3(d), respectively. Figure 3 reveals that there exists an overlap of spectra due to three types of species: (i) two magnetically inequivalent Ni^{2+} ions; (ii) Ce^{3+} spectrum (clearly present in 1% Ni doped sample only), and (iii) three kinds of O_2^- defects, very similar to those reported in the literature.[9,10] The best-fit SH parameters are listed in Table I. The two inequivalent Ni^{2+} ions occupy substitutional and interstitial sites, the spectral intensity of the latter increasing with increasing Ni^{2+} doping, such that the interstitial Ni^{2+} is present in insignificant amounts in low Ni concentration samples ($x<0.04$). Interstitial incorporation of dopants has been argued as one of the primary reasons behind the lower M_s, Curie temperature, and hole concentration in several magnetic semiconductor systems.[11,12] In light of these, it is concluded here that the gradual weakening and eventual disappearance of the FM component in $Ce_{1-x}Ni_xO_2$ samples with increasing x for $x>0.04$ are due to increasing incorporation of Ni^{2+} ions in interstitial sites. It is noted that the 8% Ni doped sample clearly showed a strong EPR signal due to the interstitial Ni^{2+} in addition to the substitutional Ni^{2+} line. The signal from interstitial Ni^{2+} sites disappeared completely when the sample was subjected to the activation process, as exhibited in Figs. 2 (bottom panel) and 3(b). This indicates that the increase in the M_s observed in the activated sample is due to the migration of some, not necessarily all, of the interstitial Ni^{2+} ions to nearby substitutional sites, so that the resulting M_s values are not in proportion to concentration (x) of Ni as our data suggest. The required energy for this is provided by the thermal energy supplied during the activation process. As for the samples with $x<0.04$, which did not show any enhancement in their FM behavior when subjected to identical activation process, there were insufficient amounts of interstitial Ni^{2+} ions to produce any further improvement in their FM due to this movement.

It is also noted that none of the EPR spectra investigated in this work displayed ferromagnetic resonance (FMR) lines. This is because the magnetization of the samples is, indeed, very small.

EPR spectral simulations on $Ce_{1-x}Ni_xO_2$ powders reveal that there are three different paramagnetic species present: (i) two Ni^{2+} at substitutional and interstitial sites, (ii) one Ce^{3+}, and (iv) three O_2^- oxygen defects. For low Ni concentrations ($x<0.04$), the Ni^{2+} ions occupy predominantly the substitutional sites, whereas for higher doping concentrations ($x \geqslant 0.04$), increased presence of interstitial Ni^{2+} ions destroy the FM. The activated samples exhibit only the spectrum for the substitutionally incorporated Ni^{2+} ion, suggesting that the slow heating process moves the interstitial ions to substitutional sites and thereby causes a dramatic increase in the FM properties.

At Boise State University, this research was supported by the NSF-CAREER award (DMR-0449639), DoE-EPSCoR grant (DE-FG02-04ER46142), NSF-Idaho-EPSCoR Program and the National Science Foundation under award No. EPS-0447689 and DMR-0321051. One of the authors (S.K.M.) is grateful to the Natural Sciences and Engineering Research Council (NSERC) of Canada for partial financial support. A portion of this research was done at the Environmental Molecular Sciences laboratory at Pacific Northwest Nation Laboratory (Richland, WA).

[1] A. Thurber, K. M. Reddy, and A. Punnoose, J. Appl. Phys. **101**, 09N506 (2007).
[2] J. M. D. Coey, M. Venkatesan, and C. B. Fitzgerald, Nat. Mater. **4**, 173 (2005).
[3] J. Philip, A. Punnoose, B. I. Kim, K. M. Reddy, S. Layne, J. O. Holmes, B. Satpati, P. R. Leclair, T. S. Santos, and J. S. Moodera, Nat. Mater. **5**, 298 (2006).
[4] E. Abi-aad, A. Bennani, J.-P. Bonnelle, and A. Aboukais, J. Chem. Soc., Faraday Trans. **91**, 99 (1995).
[5] T. L. Barr, J. Phys. Chem. **82**, 1801 (1978).
[6] St. Uhlenbrock, Ch. Scharfschwerdt, M. Neumann, G. Illing, and H.-J. Freund, J. Phys.: Condens. Matter **4**, 7973 (1992).
[7] J. van Elp, H. Eskes, P. Kuiper, and G. A. Sawatzky, Phys. Rev. B **45**, 1612 (1992).
[8] S. Deshpande, S. Patil, S. Kuchibhatla, and S. Seal, Appl. Phys. Lett. **87**, 133113 (2005).
[9] E. Abi-aad, R. Bechara, J. Grimbolt, and A. Aboukais, Chem. Mater. **5**, 793 (1993).
[10] J. B. Wang, Yu.-L. Tai, W.-P. Dow, and T.-J. Huang, Appl. Catal., A **218**, 69 (2001).
[11] W. T. Geng and K. S. Kim, Phys. Rev. B **68**, 125203 (2003).
[12] K. W. Edmonds, P. Boguslawski, K. Y. Wang, R. P. Campion, S. N. Novikov, N. R. S. Farley, B. L. Gallagher, C. T. Foxon, M. Sawicki, T. Dietl, M. B. Nardelli, and J. Bernholc, Phys. Rev. Lett. **92**, 037201 (2004).